SCIENTIFIC REPORTS

OPEN

SUBJECT AREAS:
DIAGNOSTIC MARKERS
DIAGNOSIS
LABORATORY TECHNIQUES AND PROCEDURES
CANCER PREVENTION

Received
1 May 2013

Accepted
29 August 2013

Published
17 September 2013

Correspondence and requests for materials should be addressed to X.Z.Z. (xz-zhang@whu.edu.cn)

In situ recognition of cell-surface glycans and targeted imaging of cancer cells

Xiao-Ding Xu, Han Cheng, Wei-Hai Chen, Si-Xue Cheng, Ren-Xi Zhuo & Xian-Zheng Zhang

Key Laboratory of Biomedical Polymers of Ministry of Education & Department of Chemistry, Wuhan University, Wuhan 430072, P. R. China.

Fluorescent sensors capable of recognizing cancer-associated glycans, such as sialyl Lewis X (sLe^x) tetrasaccharide, have great potential for cancer diagnosis and therapy. Studies on water-soluble and biocompatible sensors for *in situ* recognition of cancer-associated glycans in live cells and targeted imaging of cancer cells are very limited at present. Here we report boronic acid-functionalized peptide-based fluorescent sensors (BPFSs) for *in situ* recognition and differentiation of cancer-associated glycans, as well as targeted imaging of cancer cells. By screening BPFSs with different structures, it was demonstrated that $BPFS_1$ with a FRGDF peptide could recognize cell-surface glycan of sLe^x with high specificity and thereafter fluorescently label and discriminate cancer cells through the cooperation with the specific recognition between RGD and integrins. The newly developed peptide-based sensor will find great potential as a fluorescent probe for cancer diagnosis.

The over expression of specific cell-surface glycans correlated with the development and progression of many cancers[1–5], and their changes are known to affect the ability of cancer cells to grow, divide and metastasize[6,7]. For example, sialyl Lewis X (sLe^x) and sialyl Lewis A (sLe^a) tetrasaccharides are over-expressed in gastrointestinal, pancreatic, breast and hepatic cancers, and the increased expression of sLe^x is known to enhance tumor metastasis[7]. The development of sensors to rapidly detect cancer-associated glycans is of great importance for cancer diagnosis or biomarker-mediated delivery of therapeutic agents. It is extremely difficult, if not impossible, to develope specific sensor for saccharide detection since saccharide contains only one kind of recognition unit, *i.e.* hydroxyl group and lacks chromophore or fluorophore to afford signal readouts. Although some biomolecules, such as antibodies and natural lectins which can recognize saccharides with high affinity, have been used to construct saccharide biosensors[8–11], application in cancer diagnosis and therapy is much restricted due to the difficulty in synthesis, high cost, poor stability and immunogenecity[12–14]. Arising from the unique capacity of boronic acids to form boronic esters reversibly with the 1,2 and 1,3 *cis*-diols presenting on many saccharides, boronic acid-based chemosensors are now proposed for saccharide detection[15–21], due to ease of synthesis, flexibility in molecular design and inherent stability toward rigorous use. However, owing to the complexity of glycans, most of reported sensors focused on recognition of monosaccharides, not cell-surface glycans[22–24].

For *in situ* recognition of cancer-associated cell-surface glycans, the chemosensors should satisfy the criteria including ease to synthesize, good biocompatibility, ability to realize recognition at constant physiological pH in aqueous media, and glycan targeting ability with high selectivity. In this study, we tried to design a series of boronic acid-functionalized peptide-based fluorescent sensors (BPFSs). Peptides are the most versatile natural molecules with high biocompatibility and good water-solubility[25]. More importantly, since many of the receptors of bioactive peptide sequences such as arginine-glycine-aspartic acid (RGD) sequence and its receptors (integrins of $\alpha_v\beta_3$ and $\alpha_v\beta_5$)[26] are over-expressed on cancer cells, the BPFSs containing bioactive peptide sequences can simultaneously target two or more cancer biomarkers to improve the accuracy in cancer cell detection and cancer diagnosis. In fact, owing to the good water-solubility of peptides and flexibility in structure designing, boronic acid-functionalized peptides have recently become most promising agents for recognition of saccharides, including monosaccharides, oligosaccharides and cancer-associated glycans[14,27–34]. However, there is no report on BPFSs capable of *in situ* recognizing cancer-associated glycans in live cells and targeting imaging of cancer cells.

In this report, by screening a series of water-soluble and biocompatible BPFSs, we demonstrated that $BPFS_1$ with a peptide sequence of FRGDF is able to *in situ* recognize cancer-associated glycan of sLe^x with high specificity. Through the cooperation with the specific recognition between RGD sequence and its receptors, $BPFS_1$ can targetedly label and discriminate cancer cells, presenting a great potential for cancer diagnosis.

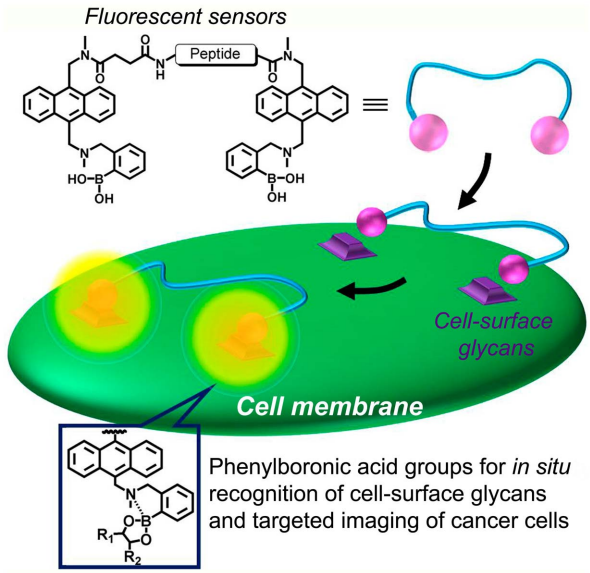

Figure 1 | **The schematic illustration of BPFSs for *in situ* cancer cell recognition and imaging.**

Results

Design, synthesis and screening of fluorescent sensors. Figure 1 shows the design principle of the fluorescent sensors for *in situ* recognition of cancer-associated glycans in live cells and targeted imaging of cancer cells. To endow the sensors with fluorescence and ability to bind with cell-surface glycans, the architecture of anthracene-phenylboronic acid was adopted[15,23,24,35–37]. In this structural motif, the anthracene fluorescence is quenched by nitrogen lone pair electrons on an amino group. However, the binding reaction between boronic acid and saccharides facilitates the formation of B-N bond, which can confine the nitrogen lone pair electrons and lead to the increase in anthracene fluorescence[15,35]. To improve the water-solubility and biocompatibility, the peptide-based linkers were employed to link two anthracene-phenylboronic acid moieties to obtain the BPFSs. Through altering the peptide sequence and length, we expect to screen and obtain the BPFSs with proper spatial arrangement of the two phenylboronic acid groups that have the potential for *in situ* recognition of cell-surface glycans with high specificity and targeted imaging of cancer cells.

Along the above design principle, five rationally designed BPFSs were synthesized (Supplementary Fig. S1–S9) and their molecular structures are shown in Figure 2A. The peptide chains of $BPFSs_{1\text{-}3}$ are comprised of five natural amino acid residues. The incorporated RGD sequences, which are capable of targeting the integrins of $\alpha_v\beta_3$ and $\alpha_v\beta_5$ over-expressed on cancer cells[26], are expected to cooperate with the phenylboronic acid groups to strengthen the targeting ability of BPFSs to cancer cells. To study the influence of peptide sequence and peptide length on the spatial arrangement of the two phenylboronic acid groups, $BPFS_4$ with a peptide sequence of FAGDF and $BPFS_5$ with a relatively long peptide sequence of FGRGDGF were also prepared together with $BPFSs_{1\text{-}3}$ to form a BPFS library.

We first evaluated the binding affinity of BPFSs with the cancer-associated glycans. Four structurally similar glycans of Lewis X (Le^x), Lewis Y (Le^y), sLe^a and sLe^x were respectively added to the PBS solution of BPFSs (1 μM, pH 7.4) and the fluorescence intensity

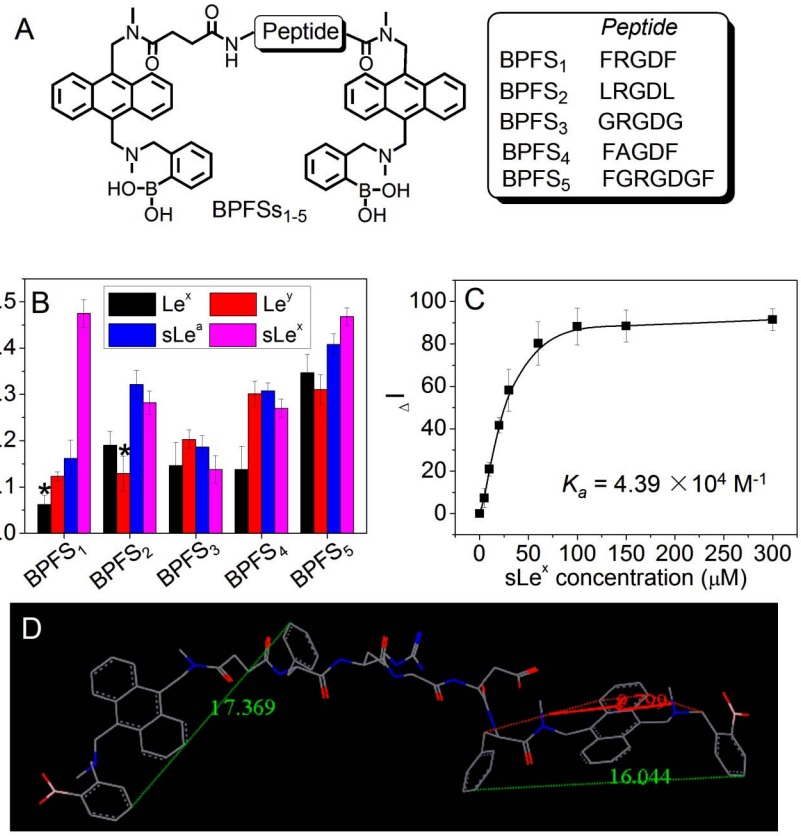

Figure 2 | (A) Molecular structures of BPFSs; (B) The maximum fluorescence intensity changes of BPFSs (1 μM) upon the addition of cancer-associated glycans of Le^x, Le^y, sLe^a and sLe^x (* means the maximum fluorescence intensity change was not observed within the used glycan concentration range from 0 to 300 μM); (C) Fluorescence intensity change of $BPFS_1$ upon the addition of different amounts of sLe^x. λ_{ex} = 370 nm, λ_{em} = 424 nm. (D) Geometry optimization of the molecular structure of $BPFS_1$ with low energy simulated by Materials studio (MS) under Dreiding force-field.

Table 1 | Selectivity factors for each BPFS screened against four different cancer-associated glycans[a]

	Le^x	Le^y	sLe^a	sLe^x
$BPFS_1$	1	1.98	2.61	7.66
$BPFS_2$	1.47	1	2.50	2.19
$BPFS_3$	1.06	1.47	1.35	1
$BPFS_4$	1	2.19	2.23	1.96
$BPFS_5$	1.16	1	1.31	1.50

[a]The fold selectivity of the BPFSs for one cancer-associated glycan over another can be obtained by dividing their respective selectivity factors.

changes were determined. These four glycans were chosen because they represent the common saccharide motifs over-expressed on cancer cells[6]. The addition of the glycans leads to the increase in the fluorescence intensity of BPFSs (Supplementary Fig. S10) and the maximum fluorescence intensity change profiles are displayed in Figure 2B. BPFSs show various fluorescence intensity changes upon the addition of the glycans, indicating different binding affinities with the glycans. In comparison with other two fluorescent sensors, $BPFS_1$, $BPFS_4$ and $BPFS_5$ having phenylalanine (Phe) residues in their peptide backbones show a relatively high affinity with one or more glycans, implying that certain interactions between Phe residues and glycans, such as the well-known CH-π interaction between the electron-deficient hydrogens on the sugar rings and π donor of electron-rich Phe[31,38], play an important role in promoting the binding of BPFSs with glycans. To compare the ability of each BPFS to differentially bind with the glycans, a selectivity factor was defined as the fluorescence intensity divided by the weakest binder induced fluorescence intensity change[33]. As presented in Table 1, $BPFS_1$ shows the optimal selectivity and a particular preference for binding with sLe^x, exhibiting more than 7-fold selectivity for sLe^x over Le^x, around 4-fold selectivity over Le^y and 3-fold selectivity over sLe^a. Here, assuming the formation of a 1 : 1 complex[39], the association constant (K_a) between $BPFS_1$ and sLe^x is calculated as around 4.39×10^4 M^{-1} from Figure 2C (the K_{as} between $BPFS_1$ and other glycans are summary in Supplementary Table S1). This high selectivity of $BPFS_1$ for sLe^x indicates its rational structural and conformational matching with sLe^x. Figure 2D displays the optimized molecular structure of $BPFS_1$. It can be found that the stereo distances between the phenyl of Phe residues and phenylboronic acid groups on $BPFS_1$ are shorter than other BPFSs (Supplementary Fig. S11). More importantly, owing to the extremely small dihedral (~9.8°) between the plane of anthracene-methylene linked to the phenyl of Phe residue and the plane of anthracene-methylene linked to the phenylboronic acid group, the phenyl and phenylboronic acid with a stereo distance of around 16 Å are nearly stretched along the same side of anthracene. This unique conformation will facilitate the specific binding of $BPFS_1$ with the glycan with a proper size to form stable interaction with phenyl. From the molecular size of the glycans (Supplementary Fig. S11), the size of Le^y (~14.4 Å) and sLe^x (~20.3 Å) is close to the distance described above (~16 Å). Although the molecular size of Le^y is smaller than that of sLe^x, its molecular structure is more rigid because all the structural units are 6-membered rigid sugar rings (Supplementary Fig. S12), which is not favor of the stereo rotation of the bound Le^y to form interaction with phenyl. However, if $BPFS_1$ binds with the sialic acid structural unit of sLe^x (Supplementary Fig. S12), the bound sLe^x could rotate relatively easily to form interaction with the phenyl of Phe residue. The selectivity mechanism based on structural simulation and optimization is further proved by the addition of another four tetrasccharides (maltotetraose, neocarratetraose, lacto-*N*-tetraose and tetra-*N*-acetyl chitotetraose, Supplementary Fig. S13). In comparison with binding with sLe^x, $BPFS_1$ shows no obvious selectivity for these four glycans (Supplementary Fig. S14).

Cell selection and expression of cancer-associated glycans. The results of BPFS screening show that $BPFS_1$ can specifically recognize sLe^x with high selectivity. Owing to the presence of bioactive RGD sequence on the peptide backbone of $BPFS_1$, it theoretically shows dual-targeting functions for cancer cells, *i.e.* phenylboronic acid group for specifically binding with the cancer-associated glycan of sLe^x and RGD sequence for specifically binding with the cancer-associated integrins of $\alpha_v\beta_3$ and $\alpha_v\beta_5$. Therefore, the human hepatic cancer cell line of HepG2 with over-expressed glycan of sLe^x and integrins was chosen to examine the ability of BPFS1 for *in situ* cell recognition and targeted imaging[40,41]. For comparison, another three cell lines, Hep3B, HT-29 and COS7, were also studied. As the hepatoma-derived cell line, Hep3B cells have been reported to express high level of glycan of Le^y [42]. HT-29 cells, as human colon cancer cells, were chosen due to their reported high expression of the cancer-associated glycan of sLe^a [4]. The COS7 cells were used because of their extremely low expression of cancer-associated glycans and integrins[24].

Flow cytometry was employed to quantitatively determine the expression of the cancer-associated glycans and integrins on these chosen cell lines. Five monoclonal antibodies of anti-sLe^x (CSLEX-1 and KM93), anti-sLe^a (CSLEA-1), anti-Le^y, anti-SSEA-1 (anti-Le^x) and anti-CD61 (labelling integrin β_3 subunit) were respectively used to stain the cells. Another monoclonal antibody of anti-CD18 was used as negative control since there is low level of corresponding antigen (integrin β_2 subunit) expressed on the chosen cell lines[4,24]. Figure 3 shows the detailed expression of the cancer-associated glycans and integrin β_3 subunit on the chosen cell lines. Except HT-29 cells that reported to express low level of integrin β_3 subunit but high level of integrin β_5 subunit[43,44], other two cancer cell lines of HepG2 and Hep3B show a much higher expression level of integrin β_5 subunit stained by anti-CD61 as compared with the normal cell line of COS7. In case of the expression of cancer-associated glycans, HepG2 cells are found to express high level of sLe^x stained by CSLEX-1 and KM93, and very low expressions of sLe^a, Le^y and Le^x. For the control cell lines, the antigen of Le^y recognized by anti-Le^y is highly expressed on Hep3B cells while the antigen of sLe^a recognized by the CSLEA-1 is highly expressed on HT-29 cells. The expressions of sLe^x, sLe^a, Le^y and Le^x are extremely low on COS7 cells.

***In situ* recognition of cell-surface sLe^x and integrins for fluorescent imaging of target cells.** After the determination of the expression of cancer-associated glycans and integrin, $BPFS_1$ was incubated with HepG2 cells to evaluate its ability to *in situ* recognize cell-surface sLe^x and integrins for fluorescent imaging of the target cells. The concentration of $BPFS_1$ used here was 20 μM because more than 85% cells were live according to the cytotoxicity assay (Supplementary Fig. S15). Figure 4 shows the confocal laser

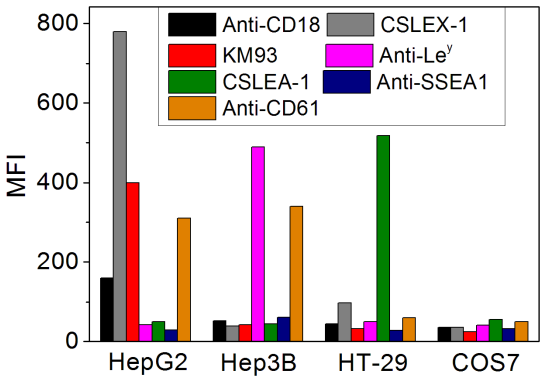

Figure 3 | Expression of the cancer-associated glycans (sLe^x, Le^y, sLe^a and Le^x) and integrin β_3 subunit on HepG2, Hep3B, HT-29 and COS7 cells determined by flow cytometry quantitative analysis.

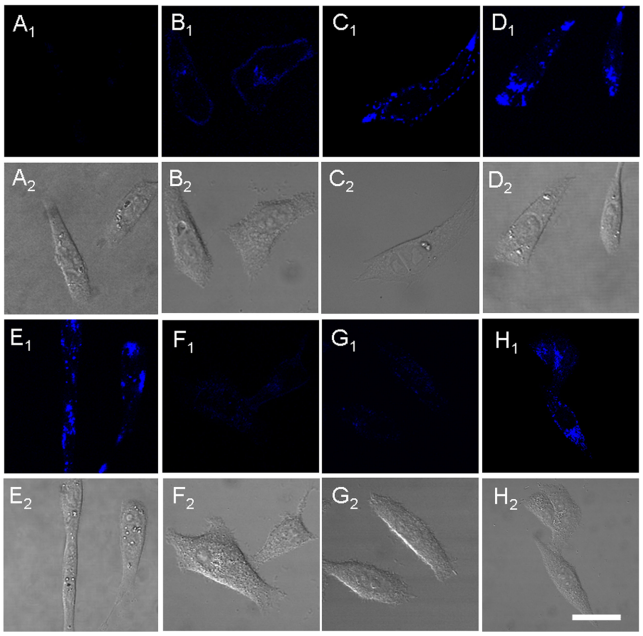

Figure 4 | (A): CLSM images of HepG2 cells incubated in free culture medium; (B–E): CLSM images of HepG2 cells incubated with $BPFS_1$ (20 μM) for 1 (B), 3 (C), 5 (D) and 10 min (E); (F): CLSM images of HepG2 cells incubated with the antibody of CSLEX-1 for 15 min and then further incubated with $BPFS_1$ (20 μM) for another 5 min; (G): CLSM images of HepG2 cells incubated with $BPFS_1$ analogue (20 μM) without phenylboronic acid groups for 10 min; (H): CLSM images of HepG2 cells incubated with $BPFS_4$ (20 μM) with a peptide sequence of FAGDF for 5 min. A_1–H_1: confocal fluorescence field images; A_2–H_2: bright field images. (The scale bar is 30 μm).

scanning microscopy (CLSM) images of the cells incubated with $BPFS_1$ for different time intervals. No fluorescence can be found for the cells incubated without $BPFS_1$ (Figure $4A_1$). After incubation with $BPFS_1$ for 1 min, besides few of internalized molecules, most of the $BPFS_1$ molecules are bound on the cell surface to form a uniform ring-shaped fluorescence pattern (Figure $4B_1$). Increasing the incubation time to 3 min, the cellular fluorescence is enhanced and the vast majority of $BPFS_1$ molecules still remain on the cell surface (Figure $4C_1$). However, after incubation for 5 min, most of $BPFS_1$ molecules have been internalized to form clusters with bright fluorescence (Figure $4D_1$). Further elongating the incubation time to 10 min does not change the distribution pattern of $BPFS_1$ molecules (Figure $4E_1$). The results of flow cytometry quantitative analysis in Figures 5A and 5C are consistent with the above CLSM observation. The mean fluorescence intensity (MFI) of the cells rapidly increases from around 480 to 1430 as the incubation time increasing from 1 to 5 min. However, there is only a slight increase in the MFI as the incubation time elongating to 10 min (MFI, around 1540). Both the CLSM observation and flow cytometry analysis indicate that $BPFS_1$ can rapidly bind with HepG2 cells and then traffic into cells, presenting the fluorescently labelling behavior. To demonstrate that the labelling behavior of $BPFS_1$ is built on the *in situ* recognition of cell-surface sLe^x and integrins, the antibody of CSLEX-1 was first incubated with HepG2 cells for 15 min and $BPFS_1$ (20 μM) was then added. As shown in Figure $4F_1$, although the recognition between CSLEX-1 and cell-surface sLe^x inhibits the binding of phenylboronic acid with sLe^x, BPFS1 can still label HepG2 cells to form a ring-shaped fluorescence pattern through the recognition between RGD and its receptors. However, owing to the relative low expression level of integrin β_3 subunit compared to sLe^x as shown in Figure 3, the cellular fluorescence is rather weak (Figure 5C). In addition, the analogue of $BPFS_1$ without phenylboronic acid groups (Supplementary Fig. S16) was also incubated with HepG2 cells. From Figure $4G_1$, without the phenylboronic acid groups to recognize cell-surface sLe^x, $BPFS_1$ can also bind with cells with weak cellular fluorescence (Figure 5C). If replacing the RGD sequence of $BPFS_1$ with AGD ($BPFS_4$), the cellular fluorescence slightly decreases as displayed in Figures $4H_1$ and 5C. All these results strongly demonstrate that the specific recognition between phenylboronic acid groups and cell-surface sLe^x dominates the fluorescently labelling behavior of $BPFS_1$ while the RGD sequence could cooperate with phenylboronic acid groups to strengthen the labelling ability of $BPFS_1$.

We also investigated the influence of the solution concentration on the labelling behavior of $BPFS_1$. The HepG2 cells were incubated with $BPFS_1$ at a concentration ranging from 1 to 80 μM for 5 min and then quantitatively analyzed by flow cytometry. As shown Figure 5B and 5D, the cells can be fluorescently labelled by $BPFS_1$ and MFI gradually increases as the concentration increasing from 1 to 40 μM. However, the MFI increase is limited if further increasing the concentration to 80 μM. Based on the cellular fluorescence changes upon the addition of $BPFS_1$ with different concentrations, the association constant (K_a) between $BPFS_1$ and cell-surface sLe^x can be calculated as around $1.38 \times 10^5\ M^{-1}$ (Figure 5D). Combining the labelling behavior under different incubation times, the optimal labelling effect of $BPFS_1$ for HepG2 cells can be achieved when incubating the cells with $BPFS_1$ (40 μM) for 5 min. If further increasing the incubation time or the concentration, there is no obvious increase in the cellular fluorescence intensity. This result implies that self-quenching behavior does not appear for the cell bound $BPFS_1$ molecules since the self-quenching of fluorophores generally induces decline in the fluorescence.

Discrimination of cell lines and determination of recognition sites. To examine the ability of $BPFS_1$ to discriminate HepG2 cells from normal cells, COS7 cells were incubated with $BPFS_1$ (40 μM, 5 min). From the CLSM image in Figure $6A_1$ and flow cytometry profile in Figure 6D, due to the low expression of cancer-associated glycans and integrins, the cellular fluorescence (MFI, around 230) is much weaker than that of HepG2 cells incubated under the same conditions. To prove that the cellular discrimination ability of $BPFS_1$ is mainly built on the specific recognition between phenylboronic acid groups and cell-surface sLe^x but not tissue-specific, the hepatoma-derived cell line of Hep3B with over-expressed Le^y and another cell line of HT-29 with over-expressed sLe^a were studied. Under the same conditions (40 μM, 5 min), owing to the weak binding affinity of $BPFS_1$ with Le^y (Figure 2B) and the presence RGD receptors on Hep3B cell surface (Figure 3), weak cellular fluorescence (MFI, around 300) can be observed in Figure $6B_1$ and 6E. The similar result can be found for HT-29 cells (Figure $6C_1$ and 6F).

To determine the binding sites between $BPFS_1$ and cell-surface sLe^x, neuraminidase specifically catalyzing the hydrolysis of α(2,3) sialic acid linkages and fucosidase specifically catalyzing the hydrolysis of α(1,3)- as well as (1,4)-linked fucose were respectively used to incubate with HepG2 cells for 4 h. Subsequently, $BPFS_1$ (40 μM) was added and the cells were further incubated for another 5 min. From the flow cytometry profile presented in Figure 7, in comparison with the cells only incubated with $BPFS_1$ (40 μM, 5 min), the addition of neuraminidase results in around 72% decrease in MFI while the addition of fucosidase induces around 78% decrease in MFI, indicating that both sialic acid and fucose residues of cell-surface sLe^x are the binding sites for $BPFS_1$. To prove this statement, fructose (400 μM), one of the strongest 1 : 1 boronic acid binders[45–47], was employed to incubate with HepG2 cells labelled by $BPFS_1$. It is noteworthy that the effective competition can be only observed when

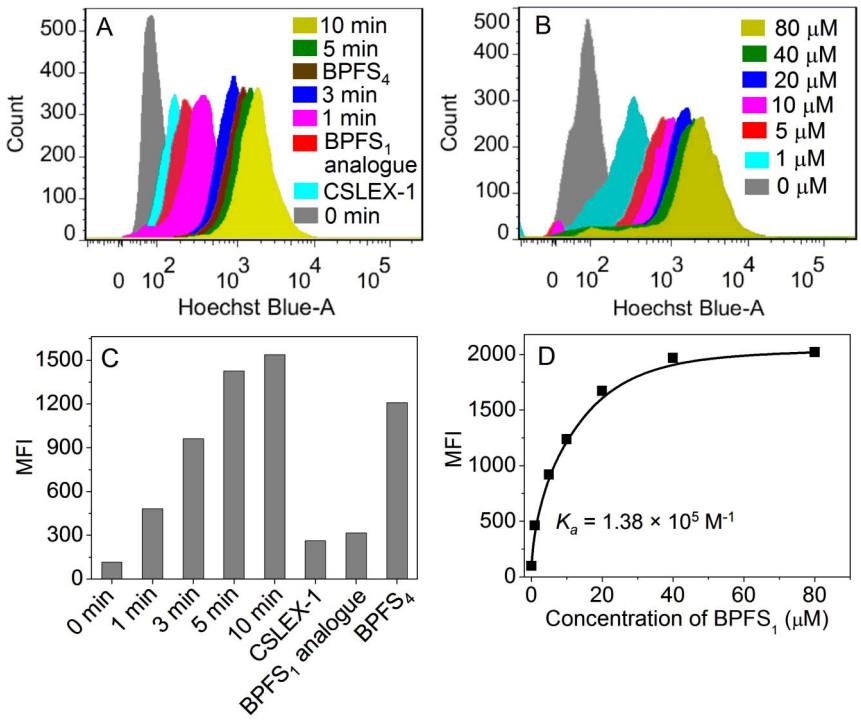

Figure 5 | **Flow cytometry profiles (A), (B) and quantification of the cellular fluorescence shown via MFI (C), (D) of HepG2 cells respectively incubated with $BPFS_1$ (20 μM) for different time (A), (C) and $BPFS_1$ at different concentration for 5 min (B), (D).**

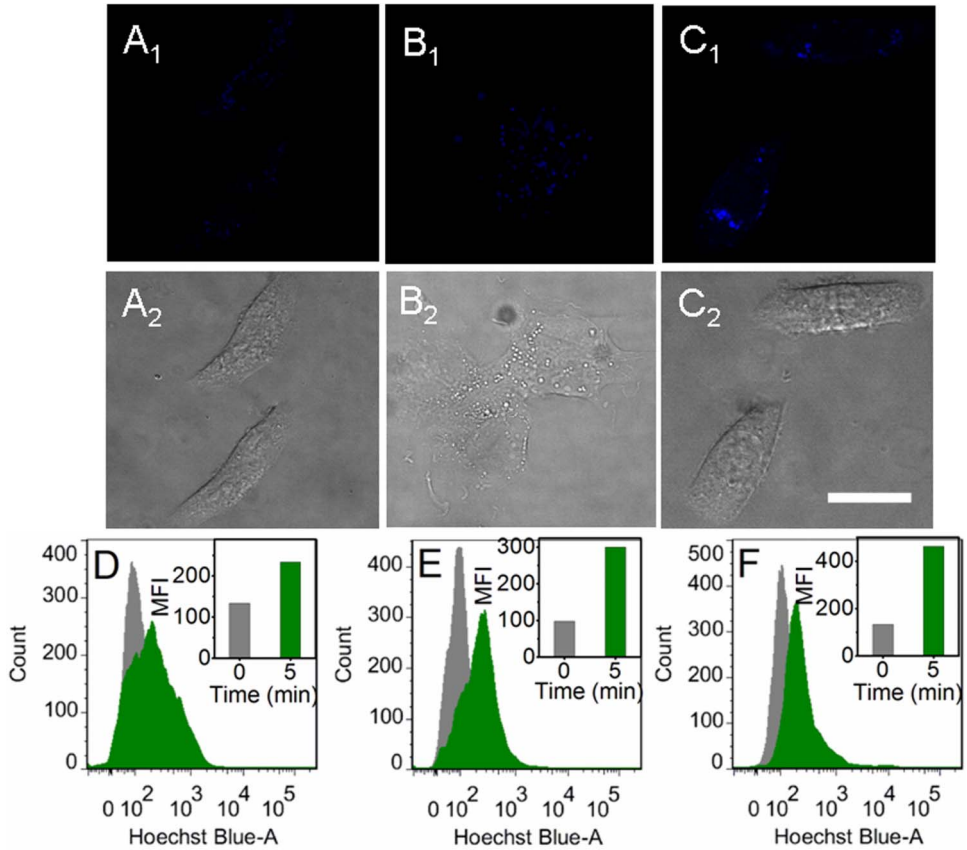

Figure 6 | CLSM images (A–C) and flow cytometry profiles (D–F) of COS7 (A), (D), Hep3B (B), (E) and HT-29 (C), (F) cells incubated with $BPFS_1$ (40 μM) for 5 min. A_1–C_1: confocal fluorescence field images; A_2–C_2: bright field images. (The scale bar is 30 μm).

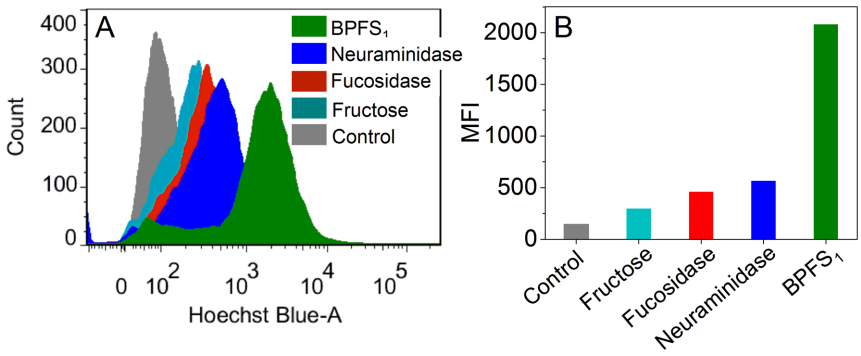

Figure 7 | Flow cytometry profiles (A) and quantification of the cellular fluorescence shown via MFI (B) of HepG2 cells incubated with $BPFS_1$ (40 μM) for 5 min ($BPFS_1$), incubated with neuraminidase for 30 min and then further incubated with $BPFS_1$ (40 μM) for 5 min (Neuraminidase), incubated with fucosidase for 30 min and then further incubated with $BPFS_1$ (40 μM) for 5 min (Fucosidase), and incubated with $BPFS_1$ (40 μM) for 5 min and then further incubated with fructose (400 μM) for 30 min (Fructose). Control represents the cells incubated without $BPFS_1$.

fructose with a high concentration (at least 10-fold excess compared to $BPFS_1$ concentration) is added. The possible reason is that the monosaccharide of fructose poorly competes with the multi-saccharides of cell-surface sLe^x since the multivalent interactions are nearly stronger than the sum of monovalent interactions[33,48]. As shown in Figure 7B, because the competitive reaction between fructose and sLe^x with $BPFS_1$ leads to the shedding of the cell bound $BPFS_1$ molecules, there is around 85% decrease in MFI after 30 min incubation. With respect to the residual cellular fluorescence, it mainly corresponds to the cell bound $BPFS_1$ molecules via the interaction between RGD segments and the receptor of integrins, which is in agreement with the CLSM observation in Figures $4F_1$ and $4G_1$. The results of enzymatic hydrolysis and fructose competition not only provide the information for the binding sites of $BPFS_1$ with cell-surface sLe^x, but quantitatively indicate the influence of RGD sequence on the binding affinity of $BPFS_1$ with sLe^x. From the Figure 7B, with addition of neuraminidase to hydrolyze sialic acid linkage of sLe^x into Le^x, the cellular fluorescence shows a 3.6-fold decrease, which is lower than decreased value (7.7-fold) revealed in Figure 2B, implying that the interaction between RGD sequence and its receptors could improve the binding affinity of phenylboronic acid group with cell-surface sLe^x and thus strengthen the labelling and targeting ability of $BPFS_1$. This interesting finding provides a valuable chance to use $BPFS_1$ as probe for clinical cancer diagnosis since the dual-targeting functions of $BPFS_1$ can facilitate each other and simultaneously recognize two types of cancer-biomarkers.

Discussion

Through structure-based screening and design, our newly developed $BPFS_1$ in this work represents the first example of water-soluble and biocompatible fluorescent sensors with dual-targeting functions to *in situ* recognize and discriminate structurally similar cancer-associated glycans and cancer cell lines. Through the cooperation of the phenylboronic acid group for specifically recognizing cell-surface sLe^x and RGD sequence for recognizing its receptors, $BPFS_1$ can rapidly bind to the surface of HepG2 cells and then traffic into cells, showing the ability to targetedly and fluorescently label HepG2 cells. Our findings agree with the fact that the sialic acid containing glycans such as sLe^x are organized on the cell membrane and reside in the intracellular organelles along the exocytotic and endocytic pathways[49,50]. Owing to this sLe^x-mediated endocytosis and the interaction between RGD and its receptors to enhance the stability of the complex between $BPFS_1$ and sLe^x, the binding affinity of $BPFS_1$ for sLe^x on cell surface ($K_a = 1.38 \times 10^5\ M^{-1}$, see Fig. 5D) is much stronger than that in an aqueous medium ($K_a = 4.39 \times 10^4\ M^{-1}$, see Fig. 2C). To fully understand the structural features of $BPFS_1$ that induce the specific recognition of cell-surface sLe^x, more computational and conformational work is needed. It is known that over-expression of sLe^x has been found in chronic inflammatory diseases of the liver and thus regarded as one of the most important biomarkers for hepatic cancers[40,41]. For clinical cancer diagnosis, the diagnostic accuracy will be significantly improved if combining the recognition of sLe^x with other cancer-associated biomarkers. Owing to the dual-targeting functions of $BPFS_1$, *i.e.* phenylboronic acid group for recognition of cancer-associated sLe^x and RGD sequence for recognition of cancer-associated integrins of $\alpha_v\beta_3$ and $\alpha_v\beta_5$, our results suggest that it can be considered as useful fluorescent probe with high accuracy for cancer diagnosis. Further development along this line could lead to a number of small molecule fluorescent probes that can be used for cell labeling, drug delivery and selective imaging applications.

Methods

Materials. The cancer-associated glycans (sLe^x, sLe^a, Le^y and Le^x) and monoclonal antibodies (anti-sLe^x, anti-sLe^a, anti-Le^y, anti-Le^x and anti-CD61) stored in PBS buffer were purchased from Sigma-Aldrich. Modified Eagle's Medium (DMEM), 3-[4,5-dimethylthiazol-2-yl]-2,5-diphenyltetrazoliumbromide (MTT), fetal bovine serum (FBS), trypsin and penicillinestreptomycin were purchased from Invitrogen Corp.

Chemical synthesis. Details of the synthesis of BPFSs are shown in Supplementary data.

Screening of BPFSs. Fluorescence spectroscopy was used to determine the affinity and selectivity of each BPFS for the cancer-associated glycans. The PBS solution of each BPFS at a concentration of 1 μM was prepared and the fluorescence emission spectra with the addition of different amount of glycans were recorded on a LS55 luminescence spectrometry (Perkin-Elmer) with excitation at 370 nm and emission data range between 380 and 500 nm. The BPFSs show different degree of increase in the fluorescence as the addition of the glycans and the maximum fluorescence intensity change at 424 nm were used to evaluate the selectivity of each BPFS for the cancer-associated glycans.

Determination of antigens. The cells (HepG2, Hep3B, HT-29 and COS7) were first incubated in DMEM containing 10% FBS and 1% antibiotics (penicillin-streptomycin, 10,000 U/mL) at 37°C in a humidified atmosphere containing 5% CO_2. Cells were then harvested and seeded in 24-well plate. After incubation for 24 h, l μL of monoclonal antibodies of anti-sLe^x (CSLEX-1 and KM93), anti-sLe^a (CSLEA-1), anti-Le^y, anti-SSEA-1 (anti-Le^x) and anti-CD61 stored in PBS buffer were respectively used to stain the cells for 15 min. Thereafter, the cells were washed with fresh DMEM (3 × 0.5 mL) and 2 μL of fluorescein isothiocyanate-conjugated goat anti-mouse IgM (0.1 mg/mL stored in PBS buffer) was added to stain the cells for 15 min. As a negative control, the cells were incubated with another monoclonal antibody of anti-CD18 (1 μL, 0.5 mg/mL stored in PBS buffer) for 15 min and then stained with fluorescein isothiocyanate-conjugated mouse IgG1/IgG2 (2 μL, 0.1 mg/mL stored in PBS buffer). After washing with fresh DMEM (3 × 0.5 mL), the cells were collected for flow cytometry analysis (BD FACSAria™ III, USA) with excitation at 488 nm.

Cytotoxicity assay. Based on the results of structure screening, $BPFS_1$ shows a high affinity and optimal selectivity for sLe^x. Therefore, $BPFS_1$ was chosen to evaluate its cytotoxicity by using MTT assay. In brief, the cells (HepG2, Hep3B, HT-29 and COS7) were seeded in 96-well plate and then incubated in 100 μL of DMEM

containing 10% FBS for 24 h. Thereafter, the medium was removed and 100 μL of DMEM containing $BPFS_1$ was added. After incubation for 48 h, the medium was replaced with 200 μL of fresh medium and 20 μL of MTT (5 mg/mL in PBS buffer) solution was added to each well. After incubation for 4 h, the medium was replaced by 200 μL of DMSO and the mixture was shaken at room temperature for several minutes. The optical density (OD) was measured at 570 nm with a microplate reader, model 550 (BIO-RAD, USA). The average value of four independent experiments was collected and the cell viability was calculated as: cell viability (%) = $(OD_{570\ (FS)}/OD_{570\ (control)}) \times 100$, where $OD_{570\ (control)}$ is obtained in the absence of $BPFS_1$ and $OD_{570\ (FS)}$ is obtained in the presence of $BPFS_1$.

***In situ* recognition of cell-surface sLe^x and integrins for fluorescent imaging of target cells.** The cells (HepG2, Hep3B, HT-29 and COS7) were seeded in 24-well plate and then incubated in 100 μL of DMEM containing 10% FBS for 24 h. Thereafter, the medium was removed and 200 μL of DMEM containing $BPFS_1$ was added. After incubation for a fixed period, the medium was removed. After washing the cells with fresh DMEM (3 × 1 mL), the cells were viewed under CLSM with excitation at 400 nm and collected for flow cytometry quantitative analysis with excitation at 375 nm. As a control, the $BPFS_1$ analogue of without phenylboronic acid groups and $BPFS_4$ dissolved in DMEM (20 μM) were also respectively incubated with HepG2 cells and the cells were subsequently viewed under a lasers canning confocal microscope (Nikon C1-si TE2000, Japan) with excitation at 405 nm and collected for flow cytometry quantitative analysis (BD FACSAria™ III, USA) with excitation at 375 nm.

Determination of recognition mechanism. HepG2 cells were seeded in 24-well plate and then incubated in 100 μL of DMEM containing 10% FBS for 24 h. Subsequently, the medium was removed and the cells were respectively treated with neuraminidase specifically catalyzing the hydrolysis of α(2,3) sialic acid linkages and fucosidase specifically catalyzing the hydrolysis of α(1,3)- as well as (1,4)-linked fucose according to modifications of manufacturer's protocols. After incubation for 4 h, the cells were washed with fresh DMEM (3 × 1 mL) and 200 μL of DMEM containing $BPFS_1$ (40 μM) was added. After incubating for 5 min and then washing with fresh DMEM (3 × 1 mL), the cells were collected for flow cytometry quantitatively analysis (BD FACSAria™ III, USA) with excitation at 375 nm. To examine the competition reaction between fructose and sLe^x for $BPFS_1$, HepG2 cells were first incubated in the DMEM containing $BPFS_1$ (40 μM) for 5 min. After washing with fresh DMEM (3 × 1 mL), the cells were further incubated in 200 μL of DMEM containing fructose (400 μM) for 30 min. Thereafter, the cells were washed with fresh DMEM (3 × 1 mL) and collected for flow cytometry quantitative analysis.

1. Fukuda, M. *Cell surface carbohydrates and cell development* (CRC Press, Boca Raton, 1992).
2. Fuster, M. M., Brown, J. R., Wang, L. & Esko, J. D. A disaccharide precursor of sialyl Lewis X inhibits metastatic potential of tumor cells. *Cancer Res.* **63**, 2775–2781 (2003).
3. Jorgensen, T. *et al*. Up-regulation of the oligosaccharide sialyl Lewis X: A new prognostic parameter in metastatic prostate cancer. *Cancer Res.* **55**, 1817–1819 (1995).
4. Weston, B. W. *et al*. Expression of human α(1,3)fucosyltransferase antisense sequences inhibits selectin-mediated adhesion and liver metastasis of colon carcinoma cells. *Cancer Res.* **59**, 2127–2135 (1999).
5. Engelstaedter, V. *et al*. Expression of the carbohydrate tumour marker Sialyl Lewis A, Sialyl Lewis X, Lewis Y and Thomsen-Friedenreich Antigen in normal squamous epithelium of the uterine cervix, cervical dysplasia and cervical cancer. *Histol. Histopathol.* **27**, 507–514 (2012).
6. Dube, D. H. & Bertozzi, C. R. Glycans in cancer and inflammation-Potential for therapeutics and diagnostics. *Nat. Rev. Drug Discov.* **4**, 477–488 (2005).
7. Hollingsworth, M. A. & Swanson, B. J. Mucins in cancer: protection and control of the cell surface. *Nat. Rev. Cancer* **4**, 45–60 (2004).
8. Carter, P. J. Improving the efficacy of antibody-based cancer therapies. *Nat. Rev. Immunol.* **6**, 343–357 (2006).
9. Jelinek, R. & Kolusheva, S. Carbohydrate biosensors. *Chem. Rev.* **104**, 5987–6015 (2004).
10. Wong, N. K. *et al*. Characterization of the oligosaccharides associated with the human ovarian tumor marker CA125. *J. Biol. Chem.* **278**, 28619–28634 (2003).
11. Dexlin, L., Ingvarsson, J., Frendeus, B., Borrebaeck, C. A. K. & Wingren, C. Membrane protein profiling of intact cells using recombinant antibody microarrays. *J Proteome Res.* **7**, 319–327 (2008).
12. Hudson, P. J. & Souriau, C. Engineered antibodies. *Nat. Med.* **9**, 129–134 (2003).
13. von Mehren, M., Adams, G. P. & Weiner, L. M. Monoclonal antibody therapy for cancer. *Annu. Rev. Med.* **54**, 343–369 (2003).
14. Bicker, K. L., Sun, J., Lavigne, J. J. & Thompson, P. R. Boronic acid functionalized peptidyl synthetic lectins: combinatorial library design, peptide sequencing, and selective glycoprotein recognition. *ACS Comb. Sci.* **13**, 232–243 (2011).
15. James, T. D., Sandanayake, K. R. A. S. & Shinkai, S. Chiral discrimination of monosaccharides using a fluorescent molecular sensor. *Nature* **374**, 345–347 (1995).
16. Lavigne, J. J. & Anslyn, E. V. Teaching old indicators new tricks: a colorimetric chemosensing ensemble for tartrate/malate in beverages. *Angew. Chem. Int Ed.* **38**, 3666–3669 (1999).
17. Wiskur, S. L. & Anslyn, E. V. Using a synthetic receptor to create an optical-sensing ensemble for a class of analytes: A colorimetric assay for the aging of scotch. *J. Am. Chem. Soc.* **123**, 10109–10110 (2001).
18. Wang, W., Gao, X. & Wang, B. Boronic acid-based sensors for carbohydrates. *Curr. Org. Chem.* **6**, 1285–1317 (2002).
19. Yang, W., Gao, X. & Wang, B. Boronic acid compounds as potential pharmaceutical agents. *Med. Res. Rev.* **23**, 346–368 (2003).
20. Dowlut, M. & Hall, D. G. An improved class of sugar-binding boronic acids, soluble and capable of complexing glycosides in neutral water. *J. Am. Chem. Soc.* **128**, 4226–4227 (2006).
21. Zhang, X., You, L., Anslyn, E. V. & Qian, X. Discrimination and classification of ginsenosides and ginsengs using bis-boronic acid receptors in dynamic multicomponent indicator displacement sensor arrays. *Chem. Eur. J.* **18**, 1102–1110 (2012).
22. Sugasaki, A., Sugiyasu, K., Ikeda, M., Takeuchi, M. & Shinkai, S. First successful molecular design of an artificial lewis oligosaccharide binding system utilizing positive homotropic allosterism. *J. Am. Chem. Soc.* **123**, 10239–10244 (2001).
23. Yang, W. *et al*. Diboronic acids as fluorescent probes for cells expressing sialyl Lewis X. *Bioorg. Med. Chem. Lett.* **12**, 2175–2177 (2002).
24. Yang, W. *et al*. The first fluorescent diboronic acid sensor specific for hepatocellular carcinoma cells expressing sialyl Lewis X. *Chem. Biol.* **11**, 439–448 (2004).
25. Ulijn, R. V. & Smith, A. M. Designing peptide based nanomaterials. *Chem. Soc. Rev.* **37**, 664–675 (2008).
26. Giancotti, F. G. & Ruoslahti, E. Integrin signaling. *Science* **285**, 1028–1032 (1999).
27. James, T. D. & Shinkai, S. Artificial receptors as chemosensors for carbohydrates. *Top. Curr. Chem.* **218**, 159–200 (2002).
28. Edwards, N. Y., Sager, T. W., McDevitt, J. T. & Anslyn, E. V. Boronic acid based peptidic receptors for pattern-based saccharide sensing in neutral aqueous media, an application in real-life samples. *J. Am. Chem. Soc.* **129**, 13575–13583 (2007).
29. Zou, Y., Broughton, D. L., Bicker, K. L., Thompson, P. R. & Lavigne, J. J. Peptide borono lectins (PBLs): a new tool for glycomics and cancer diagnostics. *Chembiochem* **8**, 2048–2051 (2007).
30. Jin, S., Cheng, Y., Reid, S., Li, M. & Wang, B. Carbohydrate recognition by boronolectins, small molecules, and lectins. *Med. Res. Rev.* **30**, 171–257 (2010).
31. Pal, A., Berube, M. & Hall, D. G. Design, Synthesis, and screening of a library of peptidyl bis(boroxoles) as oligosaccharide receptors in water: identification of a receptor for the tumor marker TF-antigen disaccharide. *Angew. Chem. Int. Ed.* **49**, 1492–1495 (2010).
32. Ke, C., Destecroix, H., Crump, M. P. & Davis, A. P. A simple and accessible synthetic lectin for glucose recognition and sensing. *Nat. Chem.* **4**, 718–723 (2012).
33. Bicker, K. L. *et al*. Synthetic lectin arrays for the detection and discrimination of cancer associated glycans and cell lines. *Chem. Sci.* **3**, 1147–1156 (2012).
34. Chen, C. S. *et al*. Peptide nanofibrous indicator for eye-detectable cancer cell identification. *Small* **9**, 920–926 (2013).
35. James, T. D., Sandanayake, K. R. A. S., Iguchi, R. & Shinkai, S. Novel saccharide-photoinduced electron transfer sensor based on the interaction of boronic acid and amine. *J. Am. Chem. Soc.* **117**, 8982–8987 (1995).
36. Karnati, V. R. *et al*. A glucose-selective fluorescence sensor based on boronic acid-diol recognition. *Bioorg. Med. Chem. Lett.* **12**, 3373–3377 (2002).
37. Manimala, J. C., Wiskur, S. L., Ellington, A. D. & Anslyn, E. V. Tuning the specificity of a synthetic receptor using a selected nucleic acid receptor. *J. Am. Chem. Soc.* **126**, 16515–16519 (2004).
38. Laughrey, Z. R., Kiehna, S. E., Riemen, A. J. & Waters, M. L. Carbohydrate-π interactions: what are they worth? *J. Am. Chem. Soc.* **130**, 14625–14633 (2008).
39. Fery-Forgues, S., Le Bris, M. T., Guette, J. P. & Valeur, B. Ion-responsive fluorescent compounds. 1. Effect of cation binding on photophysical properties of a benzoxazinone derivative linked to monoaza-I 5-crown-5. *J. Phys. Chem.* **92**, 6233–7237 (1988).
40. Mita, Y., Aoyagi, Y., Suda, T. & Asakura, H. Plasma fucosyltransferase activity in patients with hepatocellular carcinoma, with special reference to correlation with fucosylated species of alpha-fetoprotein. *J. Hepatol.* **32**, 946–954 (2000).
41. Fujiwara, Y. *et al*. The sialyl Lewis X expression in hepatocarcinogenesis: potential predictor for the emergence of hepatocellular carcinoma. *Hepatogastroenterology* **49**, 213–217 (2002).
42. Sasaki, M., Kono, N. & Nakanuma, Y. Neoexpression of Lewis Y antigen is a sensitive phenotypic change of the damaged intrahepatic bile ducts. *Hepatology* **19**, 138–144 (1994).
43. Bauer, K., Mierke, C. & Behrens, J. Expression profiling reveals genes associated with transendothelial migration of tumor cells: A functional role for $\alpha_v\beta_3$ integrin. *Int. J. Cancer* **121**, 1910–1918 (2007).
44. Goodman, S. L., Grote, H. J. & Wilm, G. Matched rabbit monoclonal antibodies against α_v-series integrins reveal a novel $\alpha_v\beta_3$-LIBS epitope, and permit routine staining of archival paraffin samples of human tumors. *Biol. Open* **1**, 329–340 (2012).
45. Appleton, B. & Gibson, T. D. Detection of total sugar concentration using photoinduced electron transfer materials: development of operationally stable, reusable optical sensors. *Sens. Actuator B Chem.* **65**, 302–304 (2000).
46. Arimori, S. *et al*. Modular fluorescence sensors for saccharides. *Chem. Commun.* 1836–1837 (2001).

47. Springsteen, G. & Wang, B. A detailed examination of boronic acid-diol complexation. *Tetrahedron* **58**, 5291–5300 (2002).
48. Mammen, M., Choi, S. K. & Whitesides, G. M. Polyvalent interactions in biological systems: implications for design and use of multivalent ligands and inhibitors. *Angew. Chem. Int. Ed.* **37**, 2754–2794 (1998).
49. Zeng, Y., Ramya, T. N. C., Dirksen, A., Dawson, P. E. & Paulson, J. C. High-efficiency labeling of sialylated glycoproteins on living cells. *Nat. Methods* **6**, 207–209 (2009).
50. Liu, A. *et al.* Quantum dots with phenylboronic acid tags for specific labeling of sialic acids on living cells. *Anal. Chem.* **83**, 1124–1130 (2011).

Acknowledgements

This work was supported by the National Natural Science Foundation of China (51125014, 51233003, 21204068 and 51003079), the Ministry of Science and Technology of China (2011CB606202) and China Postdoctoral Science Foundation (2012M511250).

Author contributions

X.D.X. and X.Z.Z. conceived and designed the experiments. X.D.X., H.C. and W.H.C. performed the experiments. X.D.X., X.Z.Z., S.X.C. and R.X.Z. analyzed the data and co-wrote the paper. X.D.X. and H.C. contributed equally to this work.

Additional information

Supplementary information accompanies this paper at http://www.nature.com/scientificreports

Competing financial interests: The authors declare no competing financial interests.

How to cite this article: Xu, X. *et al. In situ* recognition of cell-surface glycans and targeted imaging of cancer cells. *Sci. Rep.* **3**, 2679; DOI:10.1038/srep02679 (2013).